PERGAMON

Journal of Structural Geology 25 (2003) 1875–1882

JOURNAL OF STRUCTURAL GEOLOGY

www.elsevier.com/locate/jsg

Projection of dip data in conical folds onto a cross-section plane

O. Fernández*, E. Roca, J.A. Muñoz

Grup de Geodinàmica i Anàlisi de Conques, Dept. de Geodinàmica i Geofísica, Universitat de Barcelona, 08028 Barcelona, Spain

Received 12 January 2002; received in revised form 27 December 2002; accepted 30 January 2003

Abstract

The projection of dip data onto a section plane can be a source of errors in the relative and absolute position of data depending on the choice of projection vectors. To properly transfer data in conical folds onto a plane of section, a best-fitting cone must be defined for the fold. Dip data must be projected along the best-fit cone generatrices, which are defined individually for each dip measurement according to its orientation. For individual dip measurements on bedding in a conical fold, their corresponding generatrix can be defined as the line of tangency between bedding and the conical fold. Dip measurements on bedding not fitting an ideal conical geometry must be corrected before a valid generatrix can be calculated. Graphical procedures to obtain generatrices for individual dip data are discussed, and a new analytical method is proposed to calculate generatrices for dip measurements on bedding not fitting an ideal conical geometry. The maximum projection distance within conical folds is discussed, and a way to estimate the natural extent of conical folds is defined. The proposed methods are illustrated with data from a conical syncline in NE Spain.

Keywords: Dip data; Conical folds; Cross-section plane

1. Introduction

The construction of a cross-section requires the projection of the maximum amount of available data onto the plane of section in order to reduce uncertainties in the structural interpretation. However, the projection of data from elsewhere in the map, as well as from subsurface, onto the section plane is not trivial and is usually the main source of error during section construction. Any of the appropriate projection methods requires a first interpretation of the structure in order to extrapolate the geometry of the folded surfaces towards the plane of section or to define the orientation of the projection vector (DePaor, 1988; Groshong, 1999). This first interpretative step is performed to reduce the impact of local irregularities in the structure that are not relevant at the working scale, and to find the simplest geometry to transfer data onto the plane of section. The selected geometry will be the basis for defining the orientation of a projection vector of regional significance and constraints on the maximum projection distance.

Projection of data in folds must be done along the fold generatrix, the line whose motion through space defines a surface (e.g. Wilson, 1967; Bengston, 1980; Groshong, 1999). For a cylindrical fold a single generatrix can be defined, whose motion parallel to itself generates the folded surface (Ramsay, 1967). Therefore, in the case of cylindrical or subcylindrical folds, the projection vector to use is the fold axis (which is the same as the generatrix). For cylindrical and subcylindrical folds that do not fit an ideal cylindrical structure, a best-fit cylinder can be defined, and its fold axis can be used to project individual dip measurements onto a section plane. In this way, data projected onto the section plane preserve their relative position inside the general structure. The use of different vectors according to local features would lead to errors in the relative position of data on the section plane.

Non-cylindrical folds require a different approach. A possibility for some non-cylindrical folds is to subdivide them into smaller segments of cylindrical geometry (Langenberg et al., 1987). However, such an approach is not practical for non-cylindrical folds with conical geometry. Conical folds are folds whose geometry fits a portion of a cone. Conical folding is a common feature in the along-strike termination of folds and in regions of dome and basin interference folding (Stauffer, 1964; Ramsay, 1967; Wilson, 1967; Webb and Lawrence, 1986; Nicol, 1993). A conical geometry is defined by the rotation of a generatrix around a

* Corresponding author. Tel.: +34-9-3402-1373; fax: +34-9-3402-1340.
E-mail address: ofernand@geo.ub.es (O. Fernández).

0191-8141/03/$ - see front matter © 2003 Elsevier Ltd. All rights reserved.
doi:10.1016/S0191-8141(03)00034-8

fixed point (the cone apex), and thus its generatrix has varying orientations. The projection vector for individual dip measurements in a conical fold can be defined as the generatrix corresponding to that measurement. DePaor (1988) proposed an analytical method to individually determine the orientation of the generatrix corresponding to each dip measurement. This method takes into account the geometrical relations between the orientation of a conical surface at a certain point, the generatrix corresponding to this orientation, and the cone's axis. However, this method only yields good results when the folded surfaces perfectly fit a conical geometry. In natural examples, dip measurements can deviate from ideal conical geometries due to the presence of local irregularities or the error associated with field measurements. When the method proposed by DePaor (1988) is applied to data deviating from the ideal conical geometry, the generatrices derived for deviated data do not lie on the average cone defined by the structure, and lead to the erroneous projection of dip data.

Another consideration that arises when working with conical folds is the extension of such structures. Unlike ideal cylindrical folds, conical folds cannot extend indefinitely along the cone axis but must die out laterally (Wilson, 1967; Groshong, 1999). If a conical fold were to continue beyond its apex, a synclinal fold would become anticlinal, and vice versa. It is therefore fundamental to establish a maximum distance of projection for data, so as not to project it beyond the cone apex.

The objective of this paper is to define a projection procedure for conical folds, both in the aspects of projection-vector determination, and in the definition of the maximum distance of projection. A new method to calculate individual generatrices for dip data is proposed. This method uses an approach similar to that used in the projection of cylindrical structures. By fitting individual dip data onto the mean conical structure, it reduces errors in projection derived from irregularities in the structure and data-collecting errors. Theoretical and practical considerations are made on the extension and limits of conical folds, and a method for determining maximum projection distance is proposed.

2. Conical folds

Conical folds are folds whose geometry corresponds to the shape of a portion of a cone. Such folds are defined by the rotation of a generatrix fixed at an apex around an axis at a given semi-apical angle (Stauffer, 1964; Ramsay, 1967; Wilson, 1967; Stockmal and Spang, 1982; Groshong, 1999). For an ideal conical fold, a mean cone can be defined such that bedding at each point is tangent to the mean cone at that point. Bedding planes in an ideal conical fold contain a generatrix of the cone, and are perpendicular to a plane containing the cone axis and the generatrix (plane R; Fig. 1a).

When working with natural examples of conical folds, the first step is to determine the best-fit cone geometry. The best-fit cone geometry is defined by the cone axis, a, and the semi-apical angle, λ (Fig. 1a), and can be derived from a given set of dip measurements (Cruden and Charlesworth, 1972; Stockmal and Spang, 1982; Groshong, 1999). The best-fit cone defined for multilayer conical folds is valid for all layers in the fold, as the cone axis and semi-apical angle are the same for all layers. In a multilayer fold, each layer has its own apex, and the locus of all apices define the position and orientation of the cone axis.

In natural folds, however, not all data will fit a perfect cone geometry. Therefore, statistical analysis is the best tool to decide whether all data can be considered to form part of the same fold (Cruden and Charlesworth, 1972; Stockmal and Spang, 1982). Some folds may present a varying conical

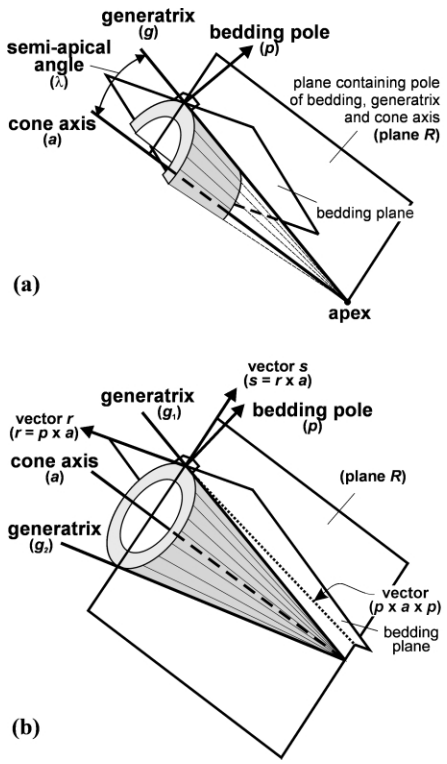

Fig. 1. (a) Graphical representation of a conical fold. The geometrical elements which define a conical fold are the generatrix (g), cone axis (a), and semi-apical angle (λ). The possible bedding orientations in such a structure are those corresponding to the planes that are tangent to the cone. All bedding planes contain the generatrix at the point of tangency, and their pole (p) is perpendicular to the generatrix. Vectors g, a and p lie on a single plane (plane R). (b) Graphical representation of the geometrical elements in the analytical method by DePaor (1988) and the method we propose. A bedding plane lying off the best-fit cone is depicted. The first cross-product for both methods yields vector r (pole to plane R). In the method by DePaor (1988) the solution (vector $p \times a \times p$, the bold dotted line) is achieved through a second cross-product. This vector lies off the cone. In our method, on the other hand, vector r is used to obtain vector **s** (a vector lying on plane R and perpendicular to the cone axis). Vector **s** is scaled and then added to the cone axis to obtain the intersections of plane R and the best-fit cone (g_1 and g_2). Of these two vectors the one forming the smallest angle with bedding is chosen as the best-fit generatrix.

geometry along the fold axis, in which case the fold should be broken down into domains in which geometry is that of a single cone.

3. Projection of data in conical folds

Projection of data in a conical fold onto a section plane should be done along the direction of the generatrix (Bengston, 1980; DePaor, 1988; Groshong, 1999). Once a maximum projection distance has been established (see Section 5), the projection of data in a conical fold onto a section plane is reduced to the problem of determining the generatrix corresponding to each dip measurement.

For data in an ideal conical fold (a fold perfectly fitting the best-fit cone), the generatrix (g) at each point will be the line of intersection of the bedding plane at that point, and a plane perpendicular to bedding containing the best-fit cone axis (plane R). The orientation of this line can be obtained graphically with the use of a stereoplot, as is shown in Fig. 2. Bengston (1980) and Groshong (1999) propose a similar graphical solution using tangent plots.

DePaor (1988) proposes an analytical solution for this method. It consists of finding the generatrix through a double cross-product of a vector parallel to the bedding pole (p) and a vector parallel to the cone axis (a):

$$g = p \times a \times p \quad (1)$$

where g is a vector parallel to the generatrix. The vectors involved in this process are depicted in Fig. 1b.

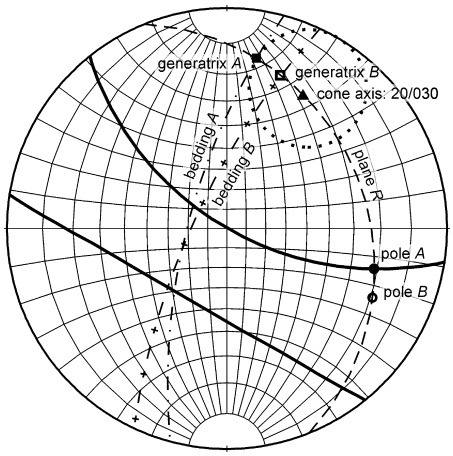

Fig. 2. Example of the determination of the generatrix for a plane in a conical fold. The bold lines are the locus of the bedding plane poles in a conical fold with axis 20/030 (solid triangle), and semi-apical angle $\lambda = 20°$. The dotted circle corresponds to the locus of the cone's generatrices (i.e. the best-fit cone). For a bedding plane A lying on the best-fit cone (bedding A dipping 285/70, dash-dot line), a plane R (dashed line) containing its pole (pole A: 20/105, solid circle) and the cone axis (20/030) is constructed. The intersection of plane R and bedding plane A yields the appropriate generatrix (generatrix A: 14/010, solid square). For a bedding plane B not lying on the best-fit cone (bedding B dipping 285/70, dash-cross line), the same procedure would yield incorrect generatrix B (17/019, empty square) lying at 11° from the cone axis, not 20°. The correct approach consists of intersecting plane R with the best-fit cone to find the bedding plane on the cone forming the smallest possible angle with plane B: plane A in this case. Plane R is then intersected with the best-fit bedding plane defined (plane A) to obtain the correct generatrix.

4. Determining projection vectors and errors for data in conical folds

Whenever a bedding plane does not lie on the best-fit cone, the vector obtained with any of the previous methods will not be a generatrix of the best-fit cone (i.e. the angle between the calculated vector and the cone axis will be different from the semi-apical angle). An example of the result of these operations for a plane not lying on the best-fit cone is shown in Figs. 1b and 2.

To avoid this problem one must follow a process similar to that used for cylindrical folds. In a cylindrical fold, the projection vector used for all data is the generatrix for the best-fit cylinder, even though individual data do not lie on this best-fit cylinder. Similarly, for data in a conical fold, the generatrix to be used should be a generatrix of the best-fit cone. For individual dip measurements the best-fit cone generatrix forming the smallest angle to the measurement should be used (DePaor, 1988).

To find the best-fit generatrix for any bedding measurement, the process to be followed is (Fig. 1b):

1. Generate plane R containing both the best-fit cone axis (a) and the pole to bedding (p);
2. Find the two lines of intersection (g_1 and g_2) of plane R with the best-fit cone. Lines g_1 and g_2 will be generatrices of the best-fit cone;
3. Of lines g_1 and g_2, the one to be used as projection vector will be that which forms the smallest angle with the original bedding.

These operations can be performed either graphically or analytically. A graphical description using a stereoplot is shown in Fig. 2.

To obtain an analytical solution, the first step is the cross product of vectors a (cone axis) and p (pole to bedding), yielding vector r (Fig. 1b):

$$r = a \times p \quad (2)$$

Vector r is the pole to plane R, which contains the cone axis and pole to bedding. The next step consists of finding a vector (vector s) perpendicular to the cone axis (a) on plane R:

$$s = r \times a \quad (3)$$

There are now two perpendicular vectors on plane R (vectors a and s). Vector s is scaled so that its length with respect to vector a is equal to the tangent of the semi-apical

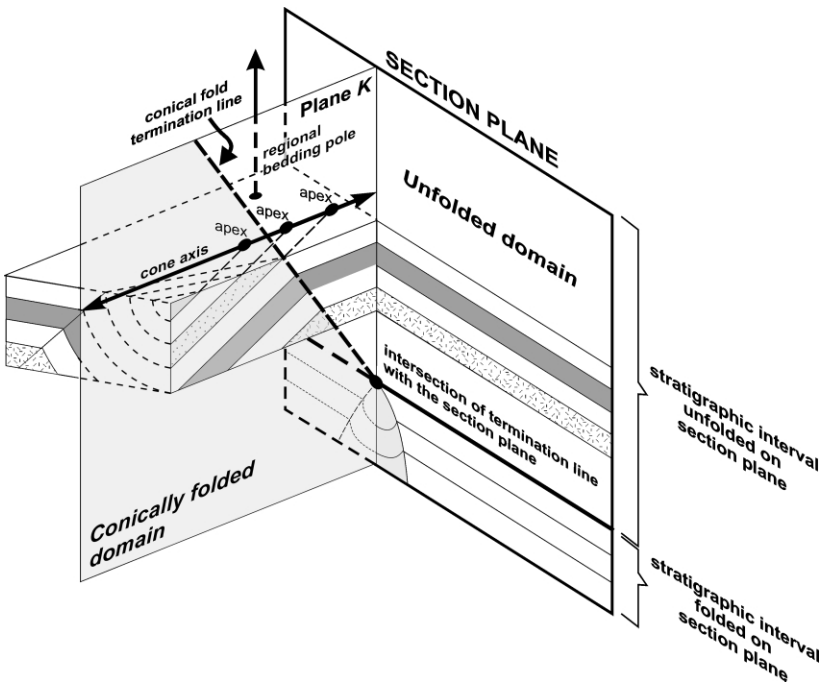

Fig. 3. Example of multilayer conical structure. Each layer has its own apex, with a common cone axis for all layers. On plane *K*, perpendicular to the regional bedding, and containing the fold axis, a termination line can be defined separating the conically folded domain from the unfolded domain. This line represents a maximum distance of projection for data in the folded domain. The area affected by conical folding is shaded. A section plane is represented which is intersected by the termination line at a certain stratigraphical position. In this case, the bedding stratigraphically above this position will not be affected by folding on the section plane. Therefore only data from lower stratigraphical levels can be projected onto the section plane from within the folded domain.

angle (λ):

$$s_{fx} = s_x \tan\lambda (a_x^2 + a_y^2 + a_z^2)^{1/2} (s_x^2 + s_y^2 + s_z^2)^{-1/2} \quad (4.1)$$

$$s_{fy} = s_y \tan\lambda (a_x^2 + a_y^2 + a_z^2)^{1/2} (s_x^2 + s_y^2 + s_z^2)^{-1/2} \quad (4.2)$$

$$s_{fz} = s_z \tan\lambda (a_x^2 + a_y^2 + a_z^2)^{1/2} (s_x^2 + s_y^2 + s_z^2)^{-1/2} \quad (4.3)$$

Where a_x, a_y, a_z, s_x, s_y, and s_z are the x, y and z components of vectors a and s; and s_{fx}, s_{fy}, and s_{fz} are the x, y and z components of the scaled vector s (s_f). If vectors a and s are of unitary length, these equations simplify to:

$$s_{fx} = s_x \tan\lambda \quad (5.1)$$

$$s_{fy} = s_y \tan\lambda \quad (5.2)$$

$$s_{fz} = s_z \tan\lambda \quad (5.3)$$

To obtain the two possible generatrices (g_1 and g_2), vector s_f is added to and subtracted from the cone axis:

$$g_1 = a + s_f \quad (6.1)$$

$$g_2 = a - s_f \quad (6.2)$$

The projection vector is the generatrix that forms the smallest angle with bedding, i.e. it lies at an angle nearest to 90° with respect to the bedding pole (p). The angle between each of the generatrices and vector p can be calculated using the dot product:

$$g \bullet p = g_x p_x + g_y p_y + g_z p_z$$

$$= (g_x^2 + g_y^2 + g_z^2)^{1/2} (p_x^2 + p_y^2 + p_z^2)^{1/2} \cos\omega \quad (7)$$

and if the length of vectors p, g_1 and g_2 have been converted to unitary length, Eq. (7) reduces to:

$$\cos\omega = g_x p_x + g_y p_y + g_z p_z \quad (8)$$

The error in the projected position for data introduced by using other projection methods instead of the proposed method is proportional to the distance of data from the section plane, and roughly proportional to the angle between the alternative projection vectors. If the section plane is vertical or nearly vertical, and the angle between the alternative projection vectors is small (under 15°), the magnitude of the error (ϵ) can be estimated by multiplying the angle (in radians) between the alternative projection vectors (β) and the distance from the data to the section plane along the projection vector direction (l; Eq. (9)):

$$\epsilon = \beta l \quad (9)$$

However, due to the fact that angle β and distance l will vary for individual dip measurements, and errors will vary accordingly, it is hard to interpret the meaning of individual errors. A possible solution is to calculate errors using only data lying farthest from the section plane to obtain an estimate of the maximum error. Alternatively, an estimate of the error can be obtained by projecting a sample of data using the proposed projection method and alternative methods onto the section plane, and analyzing the differences in the projected position of data numerically or visually.

5. Projection distance in conical folds

Once a vector of projection has been determined, a maximum distance for the projection of the data must be established. Conical folds do not extend indefinitely, but have a termination in the direction of convergence of its generatrices (Wilson, 1967; Groshong, 1999). The maximum distance of extension in this direction is its apex. For a multilayer conical structure, each layer has its own apex, and therefore its own limit (Fig. 3).

Another limitation to the along-strike extension of conical folds is imposed by the preservation of bedding thickness and continuity of bedding. For a fold terminating into a non-folded region, the intersection between the conically folded layers and non-folded layers resolves into a single line (the fold termination line; Fig. 3). The termination line can be used as a limit beyond which data within the conically folded domain cannot be projected as the conical fold terminates.

The termination line lies on a plane (plane *K*) containing both the best-fit cone axis and the pole to regional bedding, and bisects the angle between folded bedding and regional bedding on this plane (so as to preserve bedding thickness). The operations to obtain the absolute position and orientation of the termination line can be easily visualized on a plane perpendicular to regional bedding and containing the cone axis (plane *K*; Figs. 3 and 4):

1. The absolute position of the cone axis is derived from the intersection of two planes containing the cone axis and bedding poles for any two bedding planes (plane *R* as obtained with Eq. (2) in Section 4, and placed in 3D space to pass through the position of the bedding plane measurements);
2. For a certain horizon (A, for instance), the position of its apex can be obtained from the intersection of the cone axis and a bedding plane on horizon A. On plane *K* this position is obtained by extending horizon A to its intersection with the cone axis (Fig. 4a);
3. There exists a bedding plane in the unfolded domain which would contain the apex for horizon A if it were extended (horizon B; Fig. 4a);
4. For a known stratigraphical separation between horizons B and A (distance *h*), the position of horizon A can be deduced in the unfolded domain and extended to its intersection with horizon A in the folded domain (Fig. 4b). The distance (*d*) from the apex of horizon A to this intersection can be defined as a function of *h*, α (angle between regional bedding and cone axis on plane *K*), and λ (semi-apical angle), as:

$$d = \sin(\alpha + \lambda)/h \tag{10}$$

the termination line is the bisector on plane *K* of bedding in the folded and unfolded domains, placed at the intersection of folded and unfolded bedding.

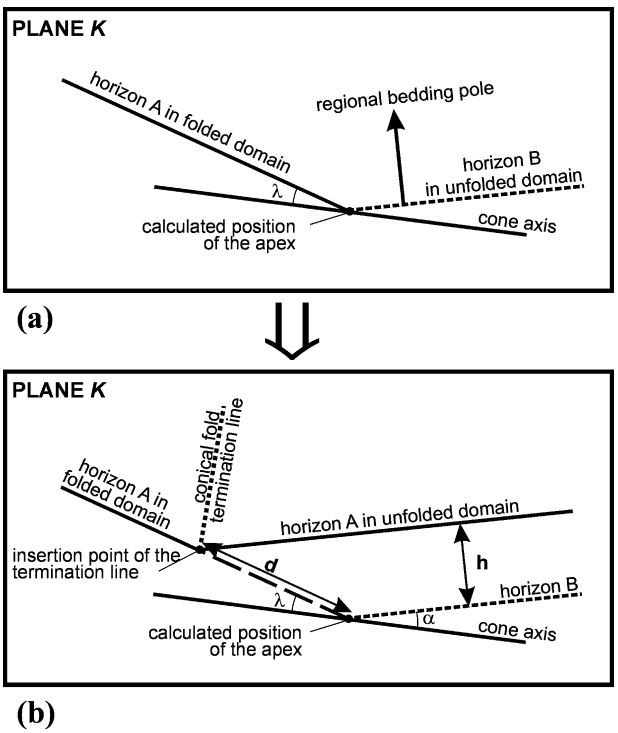

Fig. 4. Determination of the absolute position of the termination line. The illustration corresponds to a section along plane *K* (see Fig. 3). On plane *K*, the angle between the cone axis and bedding in the folded domain is equal to the semi-apical angle (λ), whereas the angle between the cone axis and unfolded bedding is α. (a) The absolute position of the apex for horizon A in the folded domain is obtained by extending bed A to the intersection with the cone axis. The horizon in the unfolded domain which contains the projected position of this apex (horizon B) is determined. (b) Horizon A in the unfolded domain is placed at a stratigraphical distance *h* from horizon B. The termination line is the bisector of bedding in the folded and unfolded domains, at distance *d* from the apex for horizon A.

The value of *d*, and the absolute position of plane *K* and of the apex for horizon A can be used to obtain the absolute position of the termination line in 3D space.[1] The termination line will intersect the section plane at a certain statigraphical horizon. Above or below this horizon bedding on the section plane will not be affected by folding (Fig. 3). Data in the folded domain can therefore be separated, according to its stratigraphical position, as data to be projected or not onto the section plane.

6. The Penyagalera syncline: an example

The Penyagalera syncline is a kilometric conical fold affecting synorogenic Tertiary conglomeratic sediments in the footwall of the frontal structure of the Catalan Coastal Ranges, in NE Spain (Lawton et al., 1999; Fig. 5). Structural analysis of 950 dip measurements of

[1] To reduce the impact of local irregularities in the position of the termination line, calculations to obtain plane *K* and the value of *d* should be repeated with different dip measurements, and an average solution derived.

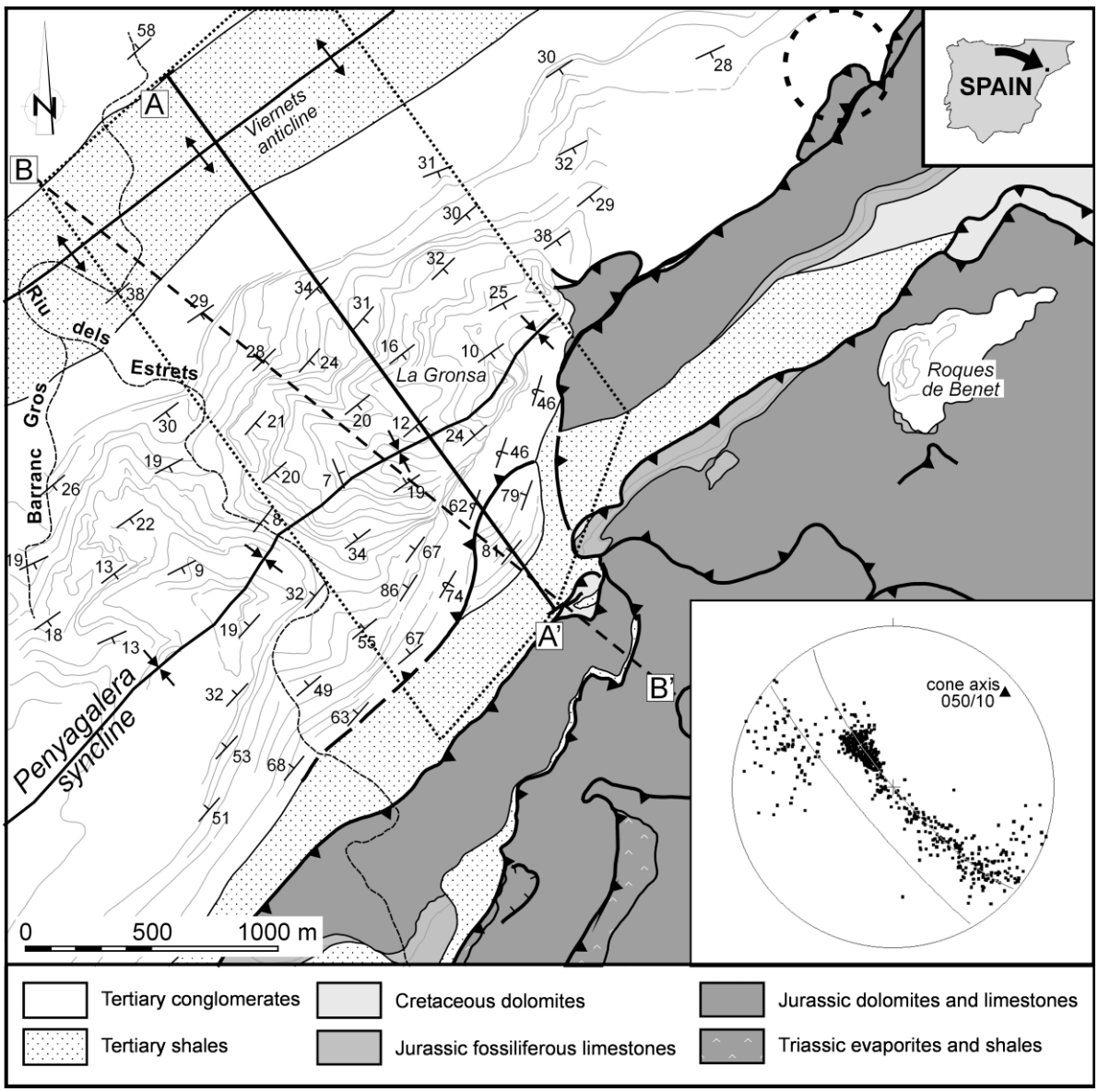

Fig. 5. Map of the Penyagalera syncline and frontal thrust structures in the southwestern sector of the Catalan Coastal Range (Modified from Lawton et al., 1999). Bold line (A–A′) indicates the position of the cross-section in Fig. 7. The dotted polygon indicates the limits of data projected onto the section in Fig. 7. The dashed circle in the northeastern sector indicates the estimated position of the cone apex for one of the highest conglomerate horizons (the size indicates uncertainty in the position). The dashed line (B–B′) shows the position of the reference cross-section (Fig. 6). Inset in the lower right corner is the stereoplot of 950 bedding poles from the Tertiary conglomerates and shales in the Penyagalera syncline. The calculated best-fit for the data is a small circle with axis plunging 10/050, and a semi-apical angle of 10°.

the Tertiary conglomerates reveals a conical geometry, with a fold axis plunging 10/050, and with a 10° semi-apical angle (Fig. 5). However, due to the syntectonic character of the conglomerates (Lawton et al., 1999), the cone axis for each horizon has a different position in space (the fold is not concentric). Thus, the position of the termination line depends on the stratigraphic horizon used for reference. To obtain a minimum estimate of the maximum projection distance, the position of the apex for the stratigraphically highest horizons was used. The position of the cone axis has been calculated for data from one of the uppermost horizons in the syncline (indicated by the bold arrow in Fig. 7c). Intersection of bedding planes on this horizon with the cone axis indicate that the position of the apex for this horizon lies far beyond the limits of the studied area (Fig. 5). Therefore, all data within the studied area can be used for projection onto the section plane.

A NW–SE vertical cross-section (A–A′) was constructed, perpendicular to the trend of the fold (Fig. 5). Six hundred and fifty dip data from the folded conglomeratic unit were projected in three different ways onto the section plane. The first projection (Fig. 7a) was done using one single projection vector (00/050), which was calculated assuming the fold to be cylindrical. The second projection

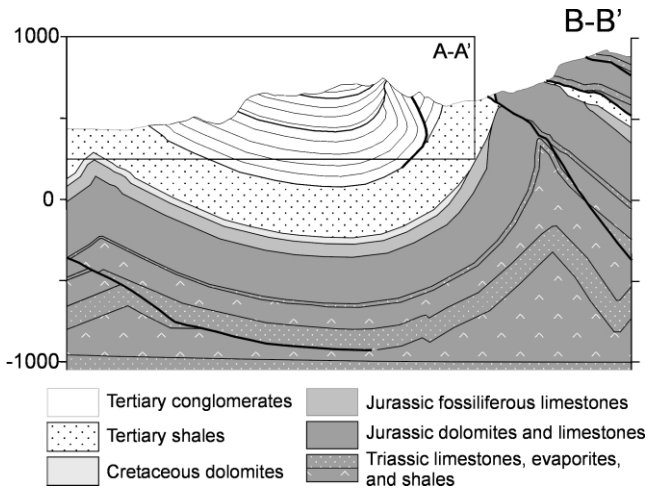

Fig. 6. Geologic cross-section (B–B′) across the Penyagalera syncline and frontal thrust structures of the Catalan Coastal Range. The box indicates the projected position of section A–A′ (Fig. 7) on section B–B′. See Fig. 5 for location. (Modified from Lawton et al., 1999.)

(Fig. 7b) was done following the method proposed by DePaor (1988), for a cone axis plunging 10/050, and 10° semi-apical angle. The third projection (Fig. 7c) was done following the steps in Section 4 for the same cone geometry. Comparison between the different results from the projection of data (Fig. 7), and with the geologic cross-section across the Penyagalera syncline (Fig. 6) reveals that data projected according to the proposed method (Fig. 7c) best fit the observed structure and correctly preserve the fold geometry.

7. Discussion

Projection of data in conical folds onto section plane must take the conical geometry into account, and should be done along the best-fit cone generatrices. The use of cone generatrices for the projection of data in conical folds permits the use of a larger data set than if the fold were partitioned into cylindrical domains. The proposed method improves existing projection methods for conical folds in that it reduces the impact of local irregularities in the

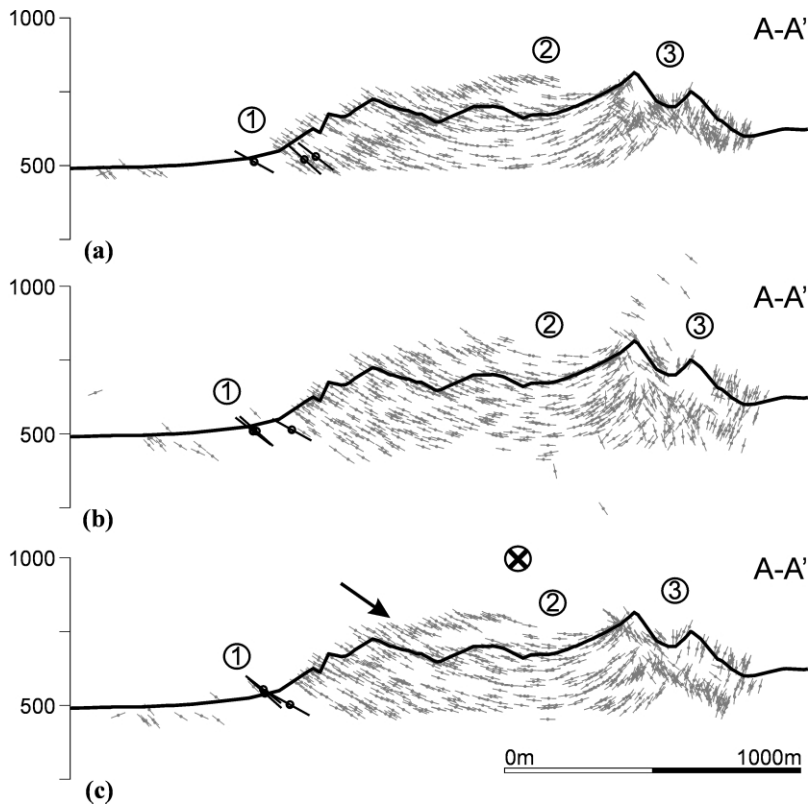

Fig. 7. Projection of 650 dip data from the Tertiary conglomerates and shales onto section A–A′ (Fig. 5). Projection has been done: (a) along a single vector (00/050); (b) according to the method by DePaor (1988) with a cone axis at 10/050; and (c) using the method proposed in this article, with a cone axis at 10/050, and semi-apical angle of 10°. The numbers indicate the main differences between sections. The most relevant differences between the three methods is indicated by numbers in the three sections. (1) indicates the position of three dip measurements (larger, black symbols) corresponding to a sandstone marker layer at the bottom of the conglomeratic sequence. The only reasonable projection is that in section (c). (2) indicates the position of the fold interlimb. Both sections (a) and (b) have data from both limbs overlapping in this zone, indicating incorrect projection. (3) corresponds to the eastern limb of the syncline where data with varying dips overlap in sections (a) and (b), whereas data in section (c) are projected coherently. The large cross in section (c) indicates the position of the cone axis calculated for one of the highest conglomerate horizons in the syncline (indicated by the arrow).

projection of data. Furthermore, the analytical resolution presented allows the automatization of the projection process, which makes it possible to work with large amounts of data.

The differences in the position of data on the section plane derived from using different projection methods will vary proportionally to the angle between the projection vectors used, and the distance from the original data to the section plane. For individual examples, data can be projected onto the section plane using the analytical methods mentioned in this article. A comparison of the results will provide an estimate of the errors introduced by using different approaches.

A correct constraining of projection distance is of great importance. Erroneous positioning of the termination of a conical fold can lead to projecting data into areas of nonexistent folding. Determination of the position of the termination line is meant as a guide, rather than a precise method, as the reliability of the result will vary depending on the degree of fit of the original data to a conical geometry. However, the implementation of such considerations is necessary to reduce the possibility of projecting structures beyond their real extents, as could happen with minor structures.

Acknowledgements

The authors wish to thank C. Kluth and A. Nicol for their constructive and useful reviews of the article, and C. Passchier for helpful comments on the final version of the manuscript. We also wish to acknowledge support from the Generalitat de Catalunya (Grup de Recerca de Geodinàmica i Anàlisi de Conques, 2001SGR-000074) and from the MCyT (Proyecto PGC BTE2000-0571, REN2001-1734-C03-03, and BTE2001-3650). Research by Oscar Fernández is funded by a pre-doctoral grant from the Direcció General de Recerca (Generalitat de Catalunya).

References

Bengston, C.A., 1980. Structural uses of tangent diagrams. Geology 8, 599–602.

Cruden, D.M., Charlesworth, H.A.K., 1972. Observations on the numerical determination of axes of cylindrical and conical folds. GSA Bulletin 83, 2019–2024.

DePaor, D.G., 1988. Balanced section in thrust belts. Part 1: construction. American Association of Petroleum Geologists Bulletin 72, 73–90.

Groshong, R.H., 1999. 3-D Structural Geology, Springer-Verlag, Berlin.

Langenberg, W., Charleswoth, H., La Riviere, A., 1987. Computer-constructed cross-sections of the Morcles nappe. Eclogae Geologica Helvetica 80, 655–667.

Lawton, T.F., Roca, E., Guimerà, J., 1999. Kinematic evolution of a growth syncline and its implications for tectonic development of the proximal foreland basin, souteastern Ebro basin, Catalunya, Spain. GSA Bulletin 111, 412–431.

Nicol, A., 1993. Conical folds produced by dome and basin fold interference and their application to determining strain: examples from North Canterbury, New Zealand. Journal of Structural Geology 15, 785–792.

Ramsay, J.G., 1967. Folding and Fracturing of Rocks, McGraw-Hill Book Company, New York.

Stauffer, M.R., 1964. The geometry of conical folds. New Zealand Journal of Geology and Geophysics 7, 340–347.

Stockmal, G.S., Spang, J.H., 1982. A method for the distinction of circular conical from cylindrical folds. Canadian Journal of Earth Science 19, 1101–1105.

Webb, B.C., Lawrence, D.J.D., 1986. Conical fold terminations in the Bannisdale Slates of the English Lake District. Journal of Structural Geology 8, 79–86.

Wilson, G., 1967. The geometry of cylindrical and conical folds. Proceedings of the Geological Association 78, 178–210.